Mon. Not. R. Astron. Soc. **000**, 1–10 (2013) Printed 9 January 2013 (MN LATEX style file v2.2)

Detection of a radio bridge in Abell 3667

E. Carretti[1⋆], S. Brown[2,3], L. Staveley-Smith[4,5], J.M. Malarecki[4], G. Bernardi[6], B.M. Gaensler[7], M. Haverkorn[8,9], M.J. Kesteven[2], and S. Poppi[10]
[1] *CSIRO Astronomy and Space Science, PO Box 276, Parkes, NSW 2870, Australia*
[2] *CSIRO Astronomy and Space Science, PO Box 76, Epping, NSW 1710, Australia*
[3] *Department of Physics and Astronomy, University of Iowa, Iowa City, Iowa 52242*
[4] *International Centre for Radio Astronomy Research, M468, University of Western Australia, Crawley, WA 6009, Australia*
[5] *ARC Centre of Excellence for All-Sky Astrophysics*
[6] *Harvard–Smithsonian Center for Astrophysics, 60 Garden Street, Cambridge, MA, 02138, USA*
[7] *Sydney Institute for Astronomy, School of Physics A29, The University of Sydney, NSW 2006, Australia*
[8] *Department of Astrophysics/IMAPP, Radboud University Nijmegen, P.O. Box 9010, 6500 GL Nijmegen, The Netherlands*
[9] *Leiden Observatory, Leiden University, P.O. Box 9513, 2300 RA Leiden, The Netherlands*
[10] *INAF Osservatorio Astronomico di Cagliari, St. 54 Loc. Poggio dei Pini, I-09012 Capoterra (CA), Italy*

Accepted xx xx xx. Received yy yy yy; in original form zz zz zz

ABSTRACT
We have detected a radio bridge of unpolarized synchrotron emission connecting the NW relic of the galaxy cluster Abell 3667 to its central regions. We used data at 2.3 GHz from the S-band Polarization All Sky Survey (S-PASS) and at 3.3 GHz from a follow up observation, both conducted with the Parkes Radio Telescope. This emission is further aligned with a diffuse X-ray tail, and represents the most compelling evidence for an association between intracluster medium turbulence and diffuse synchrotron emission. This is the first clear detection of a bridge associated both with an outlying cluster relic and X-ray diffuse emission. All the indicators point toward the synchrotron bridge being related to the post–shock turbulent wake trailing the shock front generated by a major merger in a massive cluster. Although predicted by simulations, this is the first time such emission is detected with high significance and clearly associated with the path of a confirmed shock. Although the origin of the relativistic electrons is still unknown, the turbulent re-acceleration model provides a natural explanation for the large-scale emission. The equipartition magnetic field intensity of the bridge is $B_{\rm eq} = 2.2 \pm 0.3$ μG. We further detect diffuse emission coincident with the central regions of the cluster for the first time.

Key words: galaxies: clusters: individual: A3667 – galaxies: clusters: general – radiation mechanisms: non-thermal – acceleration of particles – shock waves – polarization.

1 INTRODUCTION

A number of galaxy clusters exhibit large scale diffuse emission up to a few Mpc scale either from the central region (radio halos) or in the periphery (radio relics). Not directly associated with the activity of individual galaxies, these sources are characterized by low-surface brightness ($\sim$ 1μJy/arcsec^2 at 1.4 GHz) and steep-spectrum[1] ($\alpha < -1$) and are proof of the existence of relativistic electrons and magnetic fields spread on large scales in the intracluster medium (ICM) (e.g., Feretti 2005; Ferrari 2008; Feretti et al. 2012). These large scale structures are related to other cluster properties in the optical and X-ray domain, and are directly connected to the cluster history and evolution (Cassano et al. 2010). Observations of the synchrotron emission shows that the radio halos are mostly unpolarized, while the peripheral relics are highly polarized (e.g., Feretti 2005).

The mechanism that (re-)accelerates the relativistic electrons is still debated, but it must occur in situ because of their short radiative lifetimes. Proposed origins of radio halos include *primary* acceleration of electrons due to turbulence (e.g. Brunetti et al. 2001; Petrosian 2001) or *secondary* production of electron/positron pairs

⋆ E-mail: Ettore.Carretti@csiro.au (EC); brown@astro.umn.edu (SB); Lister.Staveley-Smith@icrar.org (LSS); Jurek.Malarecki@icrar.org (JMM); gbernardi@cfa.harvard.edu (GB); bryan.gaensler@sydney.edu.au (BMG); m.haverkorn@astro.ru.nl (MH); Michael.Kesteven@csiro.au (MJK); spoppi@oa-cagliari.inaf.it (SP)

[1] $S(\nu) \propto \nu^{\alpha}$, with α=spectral index

(CRe$^{\pm}$) due to hadronic collisions between cosmic-ray protons (CRp) and thermal protons (e.g. Blasi & Colafrancesco 1999; Pfrommer et al. 2008). The former requires some dynamical activity like cluster mergers to generate turbulent electron re–acceleration, and is expected to turn off quickly as electrons lose energy. The latter is expected to be ubiquitous in the cluster and continuously produced lasting a cluster lifetime, as cosmic ray protons live longer than a Hubble time.

The radio relics are instead believed to be generated by shocks propagating to the cluster outskirts after a major merger (Enßlin et al. 2001), though claims have been made that some relics are caused by matter infalling from Cosmic Web filaments (e.g., Enßlin et al. 1998; Brown & Rudnick 2011).

In several clusters, there have also been detections of a "bridge" connecting a peripheral relic to the central halo. The Coma cluster, Abell clusters 512, 1300, 2255, 2744, and the cluster 1RXS J0603.3+4214 all show such bridges (Kim et al. 1989; Dallacasa et al. 2009; Venturi et al. 2012; Pizzo & de Bruyn 2009; Orrú et al. 2007; van Weeren et al. 2012). The origin of relic-halo bridges is unknown, though they are clearly related to the mechanism creating the relics. Due to their large extent, however, in situ acceleration must still be responsible for the emission. The case of 1RXS J0603.3+4214 has been suggested to be related to the turbulence behind the relic (van Weeren et al. 2012).

The galaxy cluster Abell 3667 (A3667) is an ideal laboratory to study the physics of the ICM. It is a double cluster undergoing a merger where the secondary cluster is moving at high speed mostly in the plane of the sky (Owers et al. 2009). Its redshift of 0.0556 locates it a distance of 224 Mpc. Interferometric radio observations show double relics in the NW and SE outlaying regions, though no radio-halo was previously detected coincident with the diffuse X-rays of the larger sub-cluster (Röttgering et al. 1997; Johnston-Hollitt 2003). The observational suite of radio data is still incomplete, however. Single-dish observations, essential to show the whole extent of the diffuse emission, have not been available.

Using X-ray, optical, and radio interferometric data, Finoguenov et al. (2010) interpret this system as two post merger clusters that have generated the two relics as outgoing front shocks with the secondary member heading away from the centre and following the NW shock. If this interpretation is correct, the post–shock region behind the relics are expected to generate turbulence (Kang et al. 2007; Paul et al. 2011; Vazza et al. 2011), though there is currently no direct evidence for this phenomenon.

In this paper we report the detection of new large–scale synchrotron emission in the galaxy cluster A3667 previously missed by interferometric observations (e.g. Röttgering et al. 1997). Using 2.3 GHz data of the S-band Polarization All Sky Survey (S-PASS) taken with the Parkes radio telescope and a follow-up at 3.3 GHz with the same telescope, we detect a radio bridge connecting the A3667 NW relic to the central regions of the cluster. Diffuse emission from the cluster centre is also detected. The observations are described in Section 2, results and maps in Section 3. Comparison of our maps with radio interferometric, optical, and X-ray data are discussed in Section 4 along with our interpretation of the new overall picture.

We assume $H_0 = 73$ km/s/Mpc, $\Omega_m = 0.27$, and $\Omega_\Lambda = 0.73$ as cosmological parameters throughout the paper.

2 OBSERVATIONS OF A3667

2.1 Parkes 2.3 GHz

The S-band Polarization All Sky Survey (S-PASS) is a single-dish survey of the total intensity and polarized continuum emission of the entire southern sky at 2.3 GHz. The observations have been conducted with the Parkes Radio Telescope, NSW Australia, a 64-m telescope operated as National Facility by ATNF-CASS a division of CSIRO. A description of S-PASS observations and analysis is given in Carretti (2011) and Carretti et al. (2012, in preparation). Here we report a summary of the main details.

S-PASS observations are centred at the frequency of 2300 MHz, with 256 MHz bandwidth and 512 frequency channels 0.5 MHz each. The standard Parkes S-band receiver (*Galileo*) was used with a system temperature of $T_{\rm sys} = 20$ K and beam width FHWM=8.9' at 2300 MHz. This is a circular polarization system, ideal for Stokes Q and U measurements. The Digital Filter Bank Mark 3 (DFB3) was used, recording full Stokes products. Flux calibration was done with PKS B1934-638; secondary calibration with PKS B0407-658; and polarization calibration with PKS B0043-424.

Data were binned in 8 MHz channels and, after RFI flagging, 23 subbands were used covering the ranges 2176-2216 and 2256-2400 MHz, for an effective central frequency of 2307 MHz and bandwidth of 184 MHz.

The scanning strategy is based on long azimuth scans taken in the east and the west to realise absolute polarization calibration of the data. Final maps are convolved to a beam of FWHM=10.75'. Stokes I, Q, and U sensitivity is better than 1.0 mJy/beam everywhere in the covered area. Details of scanning strategy, map-making, and final maps obtained by binning all frequency channels are presented in Carretti et al. (2012, in preparation; see also Carretti 2011). Multi–frequency maps and analysis will be presented in later papers. The confusion limit at this frequency and resolution is 6 mJy (Uyaniker et al. 1998) in Stokes I, and much lower in polarization (average polarization fraction of compact sources is lower than 2%, Tucci et al. 2004). From the Galactic synchrotron emission analysis at 1.4 GHz by la Porta (2008) we estimate a Galactic rms emission at the Galactic latitude of A3667 ($b \sim -30°$) of 8 mJy at 2.3 GHz at the beam scale.

2.2 Australia Telescope Compact Array

To aid subtraction of point sources, particularly the head–tail galaxy B2007-569, interferometric observations were taken on 2011 November 26 with the Australia Telescope Compact Array at Narrabri. The field was observed for 9 hr with the telescope in its 1.5D configuration, resulting in a nominal resolution of 18 arcsec at 2.3 GHz. Data was gathered in the frequency range 1.2–3.0 GHz, but images were made only in the S-PASS band at 2.3 GHz. 14 bands 128-MHz were used to analyse the frequency behaviour. As with

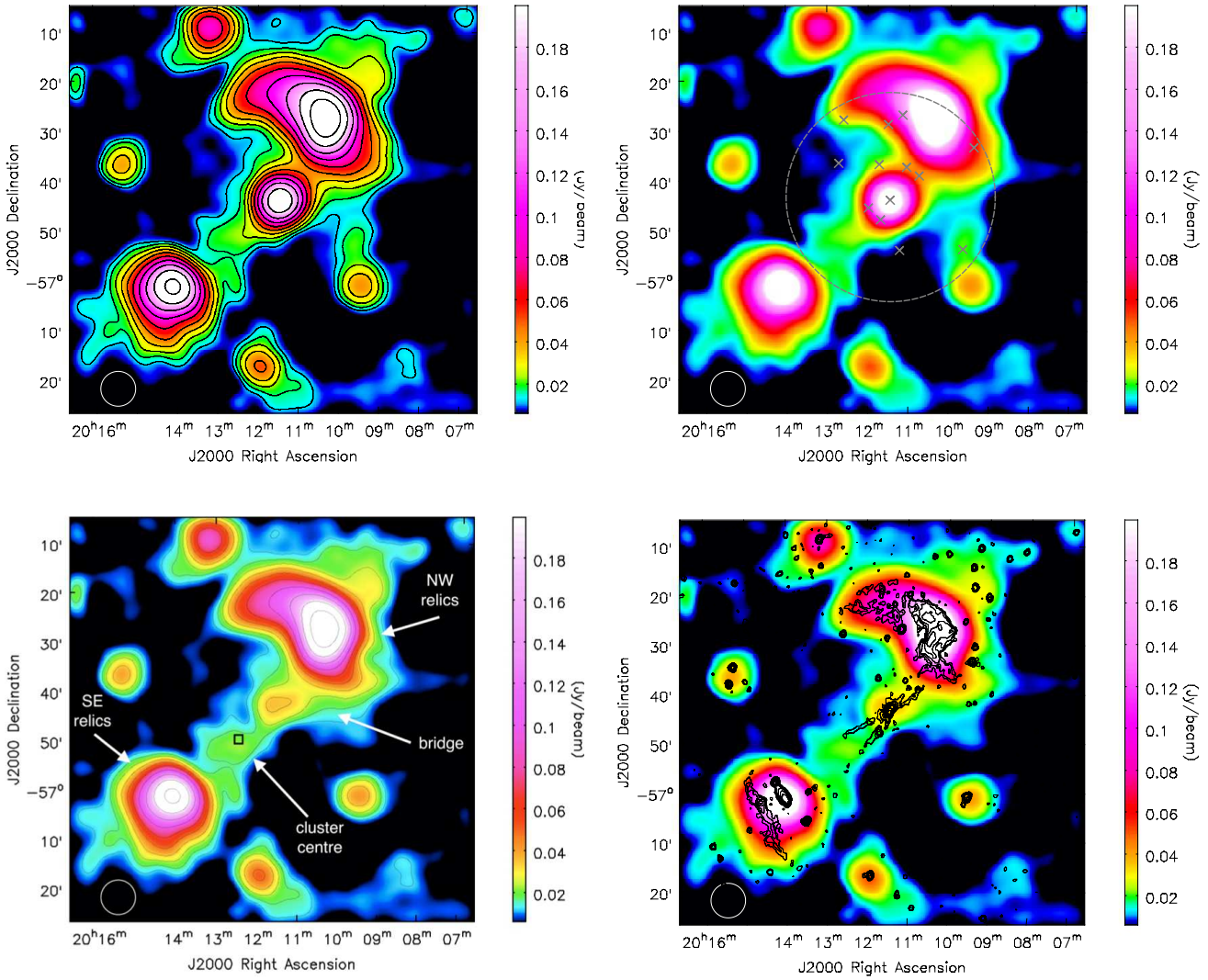

Figure 1. Top–left: Stokes I image of A3667 at 3.3 GHz taken with the Parkes radio telescope. Contour levels start from 12 mJy/beam and scale by a factor $\sqrt{2}$ thereafter. The noise budget is dominated by the confusion limit of 3 mJy. Beam size is 7.0 arcmin. **Top–right:** Same image, but with the positions of the sources detected with the ATCA observations marked (crosses). The area covered by the ATCA is also shown (gray circle). **Bottom–left:** Same figure but with B2007-569 and the other compact sources in the ATCA field subtracted. The entire area between the two relics is cleaned from compact sources. The centre of the cluster is marked with a black square and major features described in the text are labelled. **Bottom–right:** Same source–subtracted map as bottom–left panel, but with the contour levels of 843 MHz SUMSS emission overlaid. Levels start at 3 mJy/beam and scale by a factor of 2 therafter. The beam is 43" × 43" cosec(Dec).

the S-PASS observations, the flux density scale was calibrated using PKS B1934-638, to ensure the same flux scale reference for both single-dish and interferometric observations. Gaussian fits were made to the compact sources, and subtracted from the Parkes data as explained in Section 3.

2.3 Parkes 3.3 GHz

To get finer single–dish resolution and an independent confirmation of the bridge, we conducted follow up single–dish observations with the 10 cm receiver of the Parkes telescope on 2012 January 12 and 14 for a total of 6 hr. The receiver is a linear polarization system, so that only Stokes I measurements of this data set were used. Although the entire 2.6-3.6 GHz bandwidth was observed, only the top 400 MHz range centred at 3.35 GHz was used to optimise for resolution (FWHM = 5.9'). The flux density scale was again calibrated using PKS B1934-638. The DFB3 backend was used with a bandwidth of 1024 MHz and 512 frequency channels 2 MHz each. All channels of the 400 MHz sub-band were binned together. A standard basket weaving technique with orthogonal scan sets along R.A. and Dec. spaced by 2' was used to observe an area of 3° × 3° centred at the cluster. Fourier based software was applied to make the map (Carretti et al. 2010). This recovers the emission up to the scale of the area mapped, sufficient for the scales covered by the cluster (up to approximately 1°). Final maps are con-

volved to a beam of FWHM=7.0'. The sensitivity is limited by the confusion limit (3 mJy). From la Porta (2008) we estimate a Galactic rms emission at the A3667 latitude of ~ 2 mJy at 3.35 GHz at the beam scale.

3 A3667 IMAGES

Figure 1 shows the 3.3 GHz Total Intensity map centred at A3667 before compact source subtraction. The area covered with the ATCA observations and the positions of the sources found with them are also shown.

An image of the ATCA data at 2.3 GHz is shown in Figure 2. We find 13 sources with a 2.3 GHz flux density higher than 3 mJy. The central extended source is the head–tail radio galaxy B2007-569 (see close up in Figure 2), which is the bright spot between the two relics in the single-dish image. Its spectral behaviour in the ATCA band 1.2–3.0 GHz is shown in Figure 3 along with the quadratic best fitting in logarithmic space $\log S = A + B\log\nu + C\log^2\nu$, where S is the flux density and ν the frequency. The other 12 sources have been modelled with a simple power law $S \propto \nu^{\alpha}$. The flux density at 2.307 GHz (measured) and 3.350 GHz (best–fitting estimate) and spectral index are reported in Table 1. The running spectral index of B2007-569 $\alpha = d\log S/d\log\nu$ ranges from -1.0 at 1.2 GHz to -0.8 at 3.0 GHz.

Figure 1 also shows the Parkes 3.3 GHz total intensity map after source subtraction. In particular, a flux density of 219 ± 5 mJy[2] has been assumed for B2007-569. Figure 1 also shows the same image overlaid with the contour levels of the emission measured at 843 MHz by the Sydney University Molonglo Sky Survey (SUMSS, Bock, Large, & Sadler 1999).

Emission from the two relics is obvious at the NW and SE corner of the cluster and peaks at 360 and 300 mJy/beam in the 3.3 GHz Parkes data. However, no ICM emission from the central regions of the cluster is visible in the 843 MHz image. The head–tail galaxy B2007-569 can be seen to be associated with an X-shaped structure which is a SUMSS artifact not visible in other images of the same object at the same frequency (e.g. Röttgering et al. 1997).

Along with the two relics, our cleaned single-dish image shows a previously undetected radio bridge stretching for some 20' from the edge of the NW relic toward the central regions of the cluster. A second spot of diffuse emission can also clearly be seen associated with the peak of the cluster X-ray emission (see also Fig. 4). This halo seems to be connected to the second relic in the SE. Because of the resolution it is not clear whether bridge, halo, and second relic are continuous or not. If so, this would be a huge structure stretching for 60-65', corresponding to 3.9-4.2 Mpc at the A3667 distance.

The cleaned emission from the bridge ranges from 28 to 35 mJy/beam (surface brightness of 0.14-0.18 μJy/arcsec^2), a highly significant detection compared to the confusion limit. The integrated flux density is 102 ± 8 mJy.[3] The halo peaks at 22 mJy/beam with an integrated flux density of 44 ± 6 mJy. Though hints of halo emission have been seen in

[2] best fitting rms error.

[3] The error includes the B2007-569 fitting error and confusion limit.

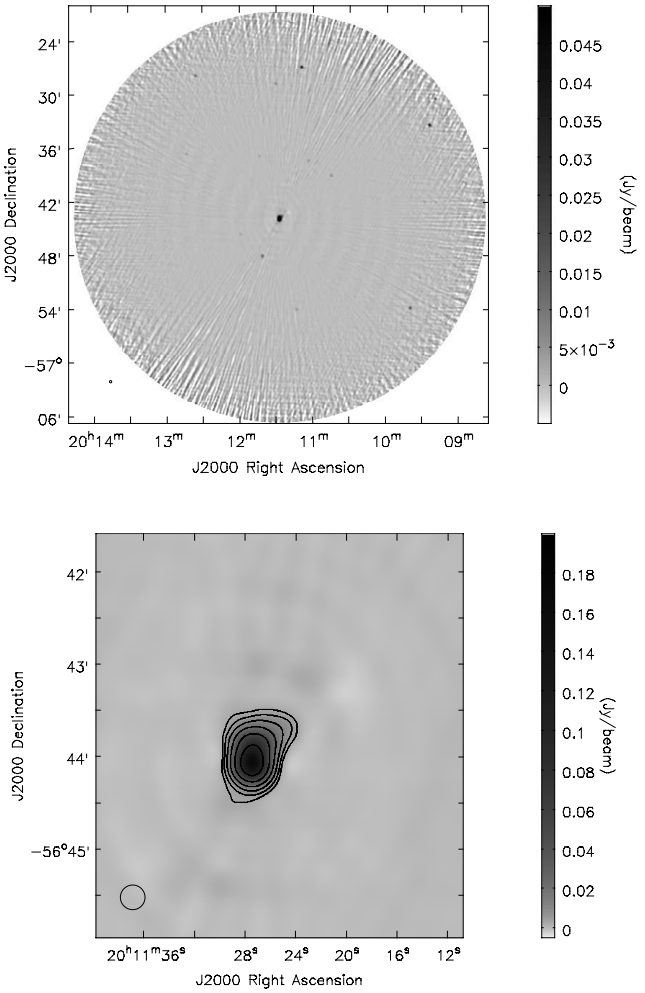

Figure 2. Top: Stokes I image of area observed with the ATCA and centred at the head–tail radio galaxy B2007-569. This image has been made using the same frequency coverage of the S-PASS observations. The rms noise is 0.3 mJy/beam. Beam size is 16 arcsec. **Bottom:** Closeup of the image focused at the head–tail radio galaxy. Contour levels start at 3 mJy/beam and scale by a factor 2.

interferometric observations, these are likely due to imaging artifacts (Johnston-Hollitt 2003). This is the first clear detection of diffuse emission coincident with the central ICM of A3667.

Figure 5 shows the 2.3 GHz S-PASS total intensity map centred at A3667 before compact source subtraction along with the position of the sources detected with the ATCA observations and the ATCA field. The flux densities measured at 2.3 GHz are reported in Table 1.

Figure 5 also shows A3667 with the ATCA field sources subtracted, including the head–tail galaxy (integrated flux density of 280 mJy). The same image overlaid with the contour levels of the 843 MHz SUMSS data is also shown. Importantly, this cleaned single-dish image clearly shows the bridge stretching for 20-25' from the edge of the NW relic

Table 1. Compact sources above 3 mJy detected in the ATCA observations.

ID	RA (J2000)	Dec (J2000)	Flux density [mJy] 2.3 GHz [c]	3.3 GHz [d]	α [a]	σ_α [b]	Notes
1	$20^h11^m27.5^s$	−56°44'04"	280	219	$-0.90+0.84\log(\frac{\nu}{2.1\mathrm{GHz}})$	$0.021\sqrt{1+304\log^2(\frac{\nu}{2.1\mathrm{GHz}})}$	B2007-569
2	$20^h12^m35.5^s$	−56°27'58"	12.9	11.4	-0.60	0.15	
3	$20^h11^m\ 9.4^s$	−56°26'58"	36.4	27.8	-0.75	0.06	
4	$20^h11^m30.4^s$	−56°28'52"	6.8	4.8	-0.70	0.22	
5	$20^h09^m25.3^s$	−56°33'27"	38.1	35.5	-0.45	0.10	
6	$20^h12^m43.1^s$	−56°36'41"	3.9	3.2	-0.76	0.14	
7	$20^h11^m43.8^s$	−56°36'58"	3.0	1.7	-1.27	0.12	
8	$20^h11^m\ 3.7^s$	−56°37'28"	5.1	3.3	-0.62	0.21	
9	$20^h10^m45.1^s$	−56°39'11"	5.4	3.6	-0.78	0.15	
10	$20^h11^m59.2^s$	−56°45'38"	3.1	2.3	-0.48	0.19	
11	$20^h11^m41.3^s$	−56°48'02"	14.4	9.5	-0.73	0.05	
12	$20^h11^m13.4^s$	−56°54'11"	4.5	3.8	-0.69	0.13	
13	$20^h09^m40.2^s$	−56°53'56"	20.0	13.0	-0.84	0.12	

[a] spectral index. For B2007-569 it is a running spectral index function of the frequency ν defined as $\alpha = d\log S/d\log\nu$
[b] rms error on α
[c] Measured
[d] Best fitting estimate

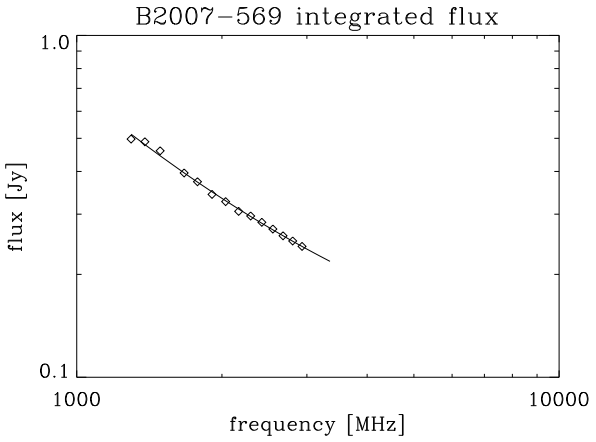

Figure 3. Integrated flux of B2007-569 (diamonds) measured in 128 MHz subbands in the 1.2–3.0 GHz range of the ATCA data. The best fitting model of the form $\log S = A + B\log\nu + C(\log\nu)^2$ is also shown (solid line).

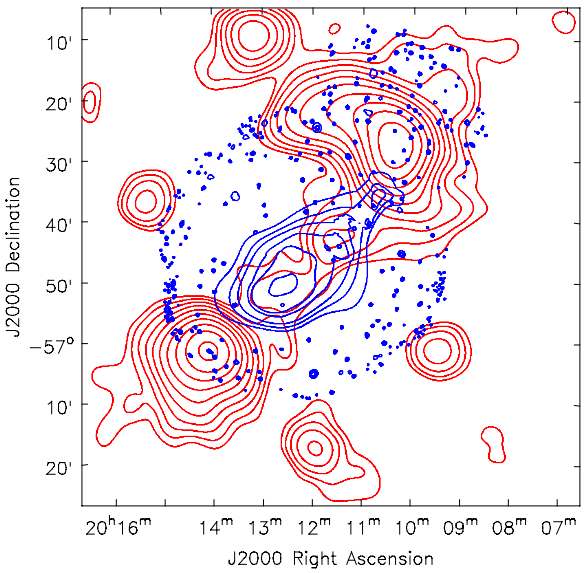

Figure 4. Contours levels of the Stokes I image of A3667 at 3.3 GHz (red) over the XMM X-ray image (blue contour levels), showing the southern extension coincident with the cluster centre. X-ray levels are 1.6, 6.4, 12.5, 25, 50, 200x10^{-6} cts/s/arcmin^2.

toward the central regions of the cluster. The cleaned emission from the bridge ranges from ∼100 to ∼115 mJy/beam, a highly significant detection. This corresponds to a surface brightness of 0.21-0.25 μJy/arcsec^2. The integrated emission is 160 ± 8 mJy. The mean spectral index from 2.3 and 3.3 GHz is $\alpha_\mathrm{b} = -1.21 \pm 0.15$. This further excludes the bridge being a residual contamination of the B2007-569 tail, whose spectrum is much steeper (spectral index between 1.4 and 2.3 GHz $\alpha_\mathrm{t} < -1.5$, Röttgering et al. 1997).

Emission from the NW and SE relics is also obvious and peaks at 750 and 460 mJy/beam, respectively.

The diffuse emission complex encompassing both the NW relic and the radio bridge covers a very extended area stretching for some 40'×40', that corresponds to 2.5 × 2.5 Mpc at the A3667 distance.

Both relics show polarized emission in our 2.3 GHz data (Figure 6). The more extended NW relic shows polarized emission centred at the total intensity peak. Its brightness is 64 mJy/beam for a polarization fraction of 8.5%. Previous observations at 1.4 GHz (Johnston-Hollitt 2003) measured 10-40% fractional polarization across the relic, though this was at high resolution with an interferometer. Toward the NE it seems to blend with more extended and weaker emission that does not appear to be associated with the cluster,

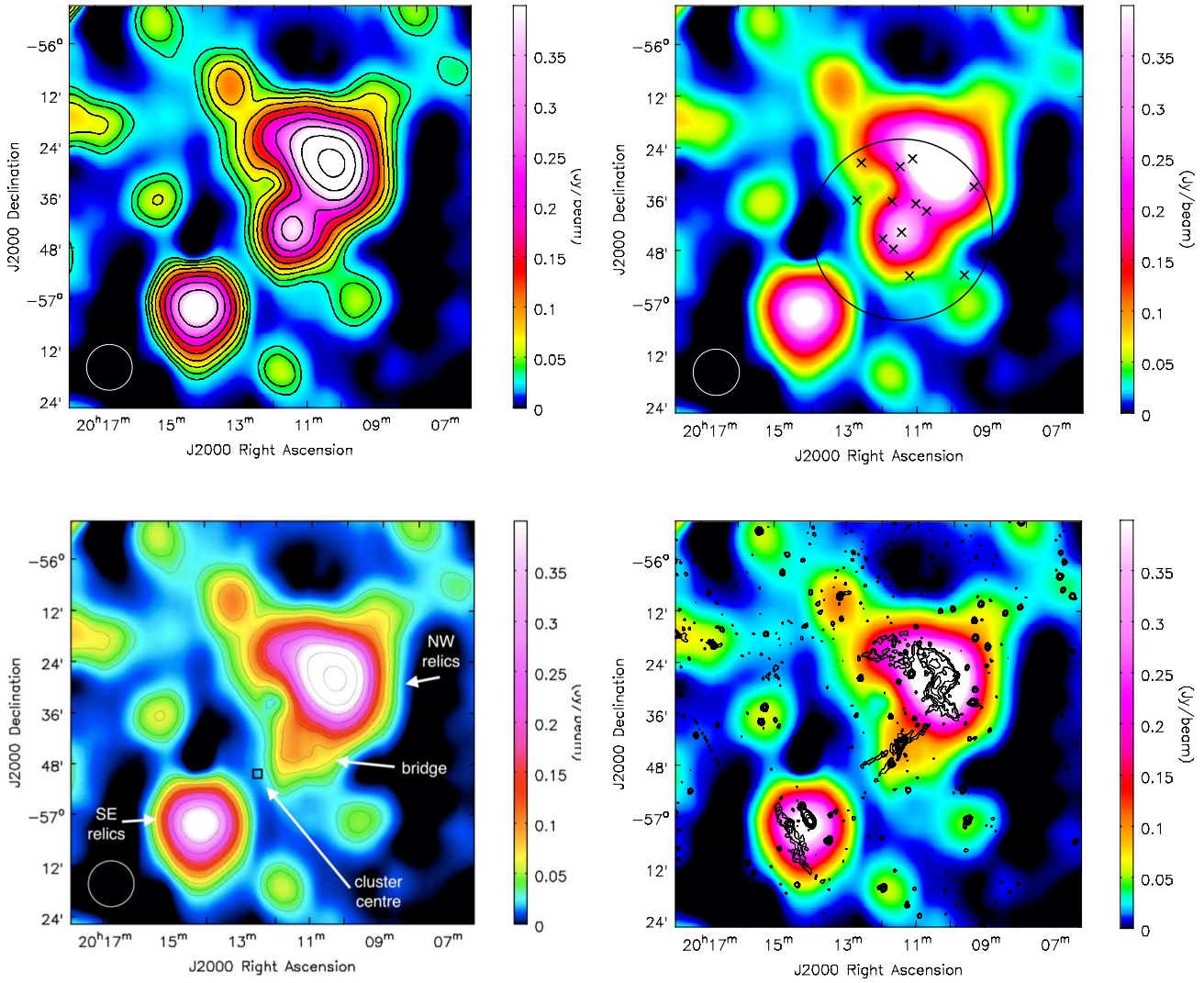

Figure 5. Top–left: Stokes I image of A3667 from S-PASS data taken at 2.3 GHz with the Parkes radio telescope. Compact sources have not been subtracted. Contour levels start from 30 mJy/beam and scale by a factor $\sqrt{2}$ thereafter. The noise budget is dominated by the confusion limit of 6 mJy. Beam size is 10.75 arcmin and reported in the bottom-left corner. **Top–right:** Same image, but with the positions of the sources detected with the ATCA observations marked (crosses). The area covered by the ATCA is also shown (black circle). **Bottom–left:** Same as above, but with the ATCA sources subtracted, including the head–tail radio galaxy B2007-569. The centre of the cluster is marked with a black square and major features described in the text are labelled. **Bottom–right:** Same source–subtracted map as bottom–left panel, but with the contour levels of the 843 MHz SUMSS emission overlaid. Levels start at 3 mJy/beam and scale by a factor of 2 thereafter. Beam is 43" × 43" cosec(Dec).

and is possibly due to Galactic foreground. This makes hard to measure the total amount of polarized emission in the NW relic.

The polarized component of the SE relic amounts to 63 mJy/beam, for a polarization fraction of 14%. The polarization angle of both relics might be subject of some Faraday Rotation. Follow–up observations at other frequencies are required.

The radio bridge does not show obvious polarized emission. An excess of 4 mJy/beam (3.5% polarization fraction) is measured compared to the surroundings, but this is likely mixed with the Galactic foreground and can be regarded as upper limit.

A small spur also seems to head NW from the NW relic, although four sources of 10-20 mJy at 843 MHz might account for this. The area was not covered in our ATCA follow up.

4 DISCUSSION

4.1 Radio interferometric data

Even higher resolution radio data for the cluster are available from SUMSS (843 MHz, see Figures 1 and 5) and the ATCA (Röttgering et al. 1997). The latter have been taken at 1.4 and 2.4 GHz, but only images at 1.4 GHz have been published. The two radio relics are obvious in those data sets

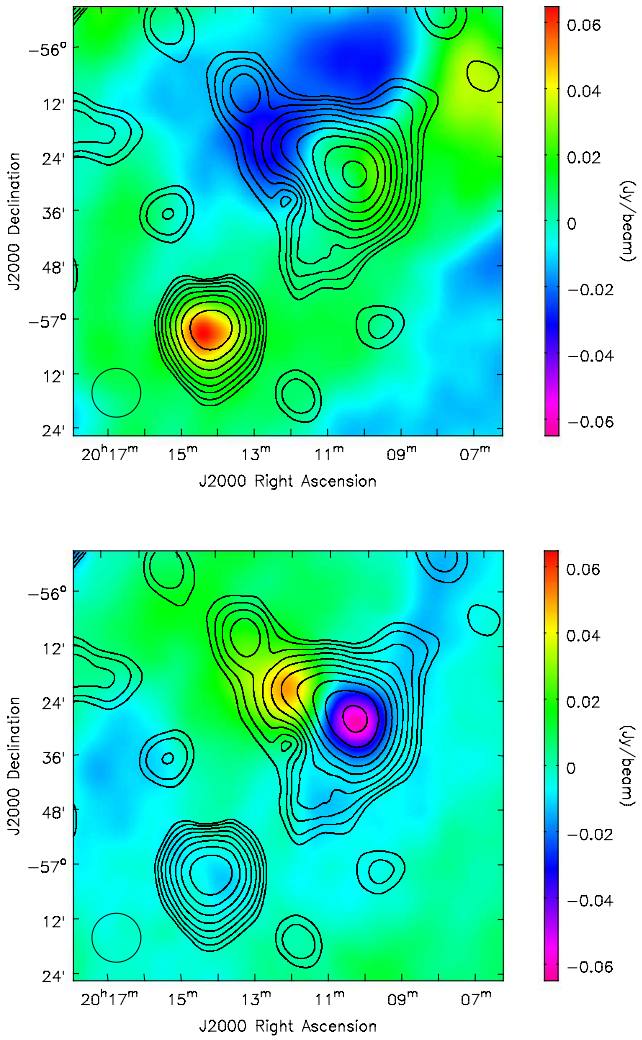

Figure 6. Stokes Q (top) and U (bottom) image of A3667 from S-PASS data taken at 2.3 GHz with the Parkes radio telescope. Stokes I contour levels as from Figure 5 are overlaid. The beam size is shown in the bottom–left corner.

and overlap well with our image. There is no trace of the bridge, except in Molonglo Observatory Synthesis Telescope (MOST) images, where there are signs of a hint of emission too noisy to be significant (Röttgering et al. 1997). The surface brightness of 0.25 μJy/arcsec^2 we detect is weaker than that usually detectable with interferometers. In addition, the emission is probably smooth with most of its power at large angular scales where the interferometers have no sensitivity.

Besides the bridge, the single–dish emission covers a more extended region than that seen by interferometer data, and results in a complex "cloud" enclosing the NW relic and the bridge, possibly stretching all the way down to the SE relic.

4.2 Comparison with optical data

Figure 7 shows the galaxy number density of A3667. Galaxies have been selected from the NASA Extragalactic Database (NED) within a distance of one degree from the

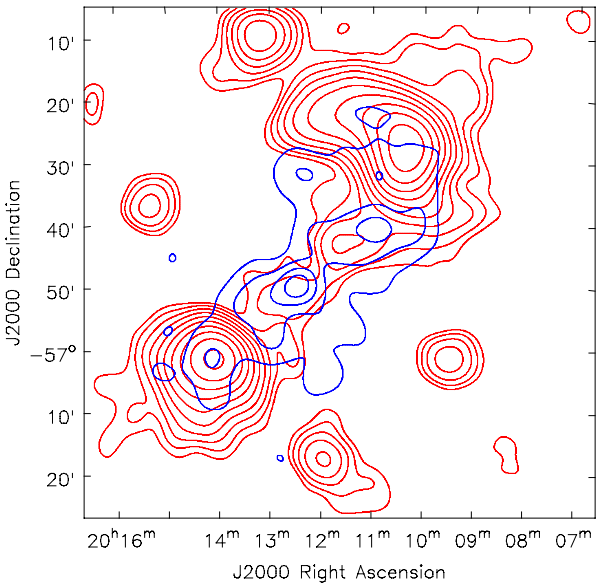

Figure 7. Contour levels of galaxy number density (blue) along with those of the 3.3 GHz source–cleaned emission of Figure 1 (red). Levels are 40, 80, 120, and 160 galaxy/Mpc^2. Galaxy positions and redshifts are from the NASA Extragalactic Database (NED).

cluster centre and within a redshift of $\Delta z = 0.01$. The latter allow separating cluster from background galaxies well (Owers et al. 2009). As found by Owers et al. (2009) there are two major peaks in the density distribution corresponding to the primary subcluster, near the A3667 centre, and to the secondary one just SE of the NW relic. While the primary subcluster is almost at rest with the overall frame of A3667, the other one looks to be moving mostly on the plane of the sky at high speed (the average line-of-sight speed is already some 500 km/s). Owers et al. (2009) interpret this structure as a post major merger cluster, with the fast moving component heading NW following the NW relic shock front.

Compared to our images, the galaxy distribution looks well aligned with the radio bridge we have detected and with the feature connecting the two relics. In particular the moving cluster appears lie near the connection between bridge and relic. There is clearly an association between the bridge and the direction of motion of both the outgoing relic and the moving subcluster.

Emission is also clearly detected at the centre of the cluster at 3.3 GHz. Only a hint is visible at 2.3 GHz, but not enough to be significant possibly because of the higher confusion limit at this frequency.

4.3 Comparison with X-ray data

Figures 4 and 8 show the X-ray emission of A3667 detected by Finoguenov et al. (2010) with XMM observations. The brightest emission is from the centre of the cluster and an extended, smooth, and weaker emission tail goes all the way to the NW relic slowly decreasing in brightness, stopping abruptly at its inner edge.

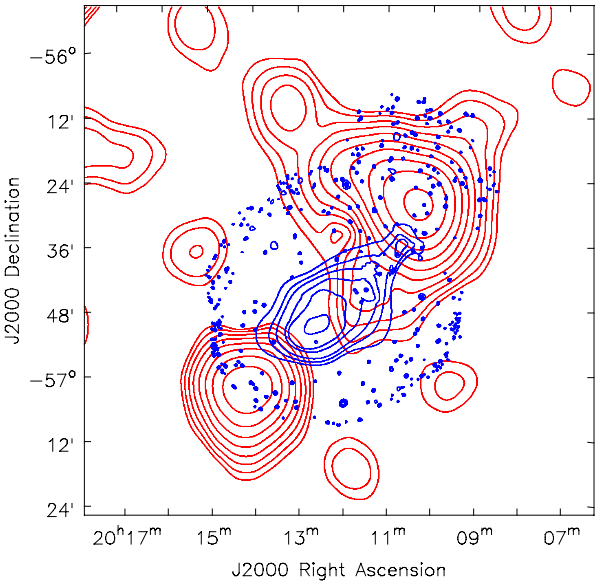

Figure 8. Contour levels of X-ray emission (blue) from XMM data (Finoguenov et al. 2010) along with those of source-cleaned Stokes I emission of Figure 5 (red). X-ray levels are 1.6, 6.4, 12.5, 25, 50, 200x10^{-6} cts/s/arcmin^2.

The radio bridge is well aligned with the X-ray tail. The two types of emission look clearly associated.

A local X-ray maximum lies close to the NW end, offset compared to the position of the moving subcluster, even though Finoguenov et al. (2010) find them associated. However, our subcluster position is consistent with that of Owers et al. (2009). We do not find obvious association between the X-ray local peak and the moving subcluster.

4.4 Interpretation

Several features distinguish the new *relic–bridge* from others seen: 1) this is one of the few double relic systems (so shocks are likely propagating in the plane of the sky) with a bridge, removing uncertainties regarding projected radio halo structures that confuse other systems; 2) there is a coincident X-ray tail detected at high significance; 3) A3667 is the only bridge in which the relic is a confirmed shock (Finoguenov et al. 2010); 4) the dynamics of the merging clusters is known very well, so we know that the bridge is "in the wake" of the passing shock.

The currently accepted interpretation is that A3667 is a post major merger cluster that has generated two outgoing shock waves (the two relics). Simulations and theoretical analysis predict that turbulence is generated in the post–shock region (Kang et al. 2007; Paul et al. 2011; Vazza et al. 2011), but no clear evidence has yet been found. Turbulence scales with thermal energies (Vazza et al. 2011), so that it is expected to be traced by enhanced X-ray emission. In A3667, the X-ray emission tail is aligned with the assumed path of the outgoing shock. Further, we clearly detect a radio bridge connecting the cluster to the NW relic and which is also aligned with the path followed by the relic, the moving cluster, and the X-ray emission tail. We conclude that the synchrotron emission is correlated to the post–shock turbulence trailing the relic shock.

The exact coupling between the turbulence and synchrotron emission could take several forms. According to turbulence re–acceleration models (e.g. Brunetti et al. 2001; Petrosian 2001), one would expect synchrotron emission to be generated in this area, assuming that the initial passage of the shock generated sufficient seed CRe$^{\pm}$. In this framework one would expect the radio emission to fade as the turbulence dissipates and the seed electrons age. The upper limit on the polarization of the bridge is consistent with no polarization, which we would expect from synchrotron emission generated in a turbulent magnetic field. The time passed since the shock wave was at the current inner edge of the NW relic can be estimated from the relic thickness (∼10') and the speed of the shock (1210 ± 220 km/s, Finoguenov et al. 2010). The resulting 0.39–0.84 Gyr (2–σ C.L.) is consistent with the time required by the turbulent re-acceleration model to reaccelerate electrons (∼0.4 Gyr with an upper limit of ∼0.7 Gyr, Cassano & Brunetti 2005) and gives sufficient time to populate the space behind the relic with synchrotron emitting electrons.

The magnetic field intensity cannot be measured directly with the data available, but an estimate can be done using the equipartition magnetic field equation from the emission intensity, spectral slope, and line-of-sight path length l (Beck & Krause 2005). From the 3.3 GHz image we measure a bridge width of 9' (beam-smearing corrected), which corresponds to 560 kpc. Assuming a cylindrical geometry (i.e. l equal to the bridge width) we compute a equipartition magnetic field $B_{\rm eq} = 2.2 \pm 0.3$ μG. We have assumed a proton-to-electron number density ratio $K_0 = 200$.[4]

An alternative explanation is that the bridge has a hadronic origin, resulting from CRp–p collisions and the resulting secondary CRe$^{\pm}$. The presence of a bridge but not a (strong) radio halo is troubling for this model, but could be due to freshly accelerated CRp (at the shock) interacting with a magnetic field strongly amplified by the post–shock turbulence (e.g. Keshet 2010), where the field may have already dissipated in the central regions. Detailed spectral-index measurements may constrain the two models.

Other interpretations for the seeding of the CRe and the generation of the turbulence are also possible, although less convincing. The relativistic electrons might in fact have been seeded by the head–tail galaxy B2007-569. However, the direction of the tails, mostly from N to N–NW (see also Figure 2 in Röttgering et al. 1997), cannot account for the direction of the bridge, whose axis is NW to W–NW. A second alternate interpretation is that the radio emission is still generated by turbulence, but caused by the motion of the fast moving subcluster. However, its position in the middle of the X-ray tail cannot account for the X-ray emission of the section between subcluster and NW relic.

In all cases, the indicators point toward the large-scale synchrotron emission being associated with post–shock turbulence generated by a major merger in a massive cluster. Although predicted by simulations (Kang et al. 2007;

[4] Typical expected values in clusters are K_0 = 100–300 (e.g. see Pfrommer & Enßlin 2004): The magnetic field estimate would vary from 1.8 to 2.4 μG within such a range.

Paul et al. 2011; Vazza et al. 2011), this is the first time such emission is detected with high significance and clearly associated with the path of a confirmed shock. This result supports a turbulent re-acceleration model for the relativistic electrons, that naturally explains the presence of a synchrotron bridge in the post–shock region.

The radio luminosity of the halo is $P_{1.4} = 7.5 \times 10^{23}$ W/Hz, extrapolated to 1.4 GHz using a spectral index of -1. With A3667's X-ray luminosity ($L_X = 9.3 \times 10^{44}$ erg/s, Reiprich & Böhringer 2002), this sets the halo between the $P_{1.4}$–L_X correlation and the *off-state* found in Brown et al. (2011b).

5 SUMMARY

We have detected a radio bridge of unpolarized synchrotron emission connecting the NW relic of Abell 3667 to the central regions of the cluster. This emission is further aligned with a diffuse X-ray tail, and represents the most compelling evidence for an association between ICM turbulence and diffuse synchrotron emission. Though the origin of the relativistic electrons is still unknown, the turbulent re-acceleration model (Brunetti et al. 2001; Petrosian 2001) provides a natural explanation for the large-scale emission. Further spectral and high-resolution observations are needed in order to differentiate this from potential hadronic secondary models of cosmic-ray acceleration in the post–shock region. We further detect diffuse emission coincident with the central regions of the cluster for the first time.

ACKNOWLEDGMENTS

This work has been carried out in the framework of the S-band All Sky Survey collaboration (S-PASS). We would like to thank Alexis Finoguenov for the electronic image of the XMM X-ray emission of A3667 and an anonymous referee for useful comments that helped improve the paper. B.M.G. acknowledges the support of an Australian Laureate Fellowship from the Australian Research Council through grant FL100100114. M.H. acknowledges the support of the research programme 639.042.915, which is partly financed by the Netherlands Organisation for Scientific Research (NWO). The Parkes radio telescope is part of the Australia Telescope National Facility which is funded by the Commonwealth of Australia for operation as a National Facility managed by CSIRO. The Australia Telescope Compact Array is part of the Australia Telescope National Facility which is funded by the Commonwealth of Australia for operation as a National Facility managed by CSIRO. We acknowledge the use of NASA Extragalactic Database.

REFERENCES

Beck R., Krause M., 2005, Astron. Nachr., 326, 414
Blasi P., Colafrancesco S., 1999, APh, 12, 169
Bock D.C.J., Large M.I., Sadler E.M., 1999, AJ, 117, 1578
Brown S., Rudnick L., 2011, MNRAS, 412, 2
Brown S., Emerick A., Rudnick L., Brunetti G., 2011, ApJ, 740, L28
Brunetti G., 2009, A&A, 508, 599
Brunetti G., Setti G., Feretti L., Giovannini G., 2001, MNRAS, 320, 365
Brunetti G., Cassano R., Dolag K., Setti G., 2009, A&A, 507, 661
Cassano R., Brunetti G., 2005, MNRAS, 357, 1313
Cassano R., Ettori S., Giacintucci S., et al. 2010, ApJ, 721, L82
Carretti E., 2011, in The Dynamic ISM: A celebration of the Canadian Galactic Plane Survey, Eds. R. Kothes, T. L. Landecker, and A. G. Willis, ASP Conf. Ser. CS-438, 276
Carretti E., Haverkorn M., McConnell D., Bernardi G., McClure-Griffiths N. M., Cortiglioni S., Poppi S., 2010, MNRAS, 405, 1670
Dallacasa D., Brunetti G., Giacintucci S., Cassano R., Venturi T., Macario G., Kassim N.E., Lane W., Setti G., 2009, ApJ, 699, 1288
Enßlin T.A., Biermann P.L., Klein U., Kohle S., 1998, A&A, 332, 395
Enßlin T.A., Gopal-Krishna, 2001, A&A, 366, 26
Feretti L., 2005, Advances in Space Research, 36, 729
Feretti L., Giovannini G., Govoni F., Murgia M., 2012, A&ARv, 20, id.54
Ferrari C., Govoni F., Schindler S., Bykov A.M., Rephaeli Y., 2008, Space Science Rev., 134, 93
Finoguenov A., Sarazin C.L., Nakazawa K., Wik D.R., Clarke T.E., 2010, ApJ, 715, 1143
Johnston-Hollitt, M. 2003, Ph.D. Thesis
Kang H., Ryu D., Cen R., Ostriker J.P., 2007, ApJ, 669, 729
Kim K.-T., Kronberg P.P., Giovannini G., Venturi T., 1989, Nature, 341, 720
Kronberg P.P., Kothes R., Salter C.J., Perillat P., 2007, ApJ, 659, 267
La Porta L., Burigana C., Reich W., Reich P., 2008, A&A, 479, 641
Orrú E., Murgia M., Feretti L., Govoni F., Brunetti G., Giovannini G., Girardi M., Setti G., 2007, 467, 943
Owers M.S., Couch W.J., Nulsen P.E.J., 2009, ApJ, 693, 901
Paul S., Iapichino L., Miniati F., Bagchi J., Mannheim K., 2011, ApJ, 726, 17
Petrosian V., 2001, ApJ, 557, 560
Pfrommer C., Enßlin T.A., 2004, MNRAS, 352, 76
Pfrommer C., Ensslin T.A., Springel V., 2008, MNRAS, 385, 1211
Pizzo R.F., de Bruyn A.G., 2009, 507, 639
Reiprich T.H., Böhringer H., 2002, ApJ, 567, 716
Röttgering H.J.A., Wieringa M. H., Hunstead R.W., Ekers R.D., 1997, MNRAS, 290, 577
Roettiger K., Burns J.O., Stone J.M., 1999, ApJ, 518, 603
Tucci M., Martínez-González E., Toffolatti L., González-Nuevo J., De Zotti G., 2004, MNRAS, 349, 1267
Uyaniker B., Fürst E., Reich W., Reich P., Wielebinski R., 1998, A&AS, 132, 401
van Weeren R.J., Röttgering H.J.A., Intema H.T., Rudnick L., Brüggen M., Hoeft M., Oonk J.B.R., 2012, A&A, 546, A124
Vazza F., Brunetti G., Gheller C., Brunino R., Brüggen M., 2011, A&A, 529, A17
Venturi T., Giacintucci S., Dallacasa D., Cassano R., Brunetti G., Macario G., Athreya R., 2012, A&A, in press,

arXiv:1210.7617

This paper has been typeset from a TEX/ LATEX file prepared by the author.